

Conductivity, calorimetry and phase diagram of the NaHSO₄–KHSO₄ system

H. Hamma^a, S.B. Rasmussen^b, J. Rogez^a, M. Alaoui-Elbelghiti^c, K.M. Eriksen^b, R. Fehrmann^{b,*}

^a Laboratoire TECSER, UMR 6122-CNRS, Faculté des Sciences et Techniques de St Jérôme, 13397 Marseille Cedex 20, France

^b Department of Chemistry and Center for Sustainable and Green Chemistry, Technical University of Denmark, DK-2800 Kgs. Lyngby, Denmark

^c Département de Chimie, Université Mohammed V-Agdal, Avenue Ibn Battouta, Rabat, Morocco

Received 24 May 2005; received in revised form 11 November 2005; accepted 11 November 2005

Available online 15 December 2005

Abstract

Physico-chemical properties of the binary system NaHSO₄–KHSO₄ were studied by calorimetry and conductivity. The enthalpy of mixing has been measured at 505 K in the full composition range and the phase diagram calculated. The phase diagram has also been constructed from phase transition temperatures obtained by conductivity for 10 different compositions and by differential thermal analysis. The phase diagram is of the simple eutectic type, where the eutectic is found to have the composition $X(\text{KHSO}_4) = 0.44$ (melting point ≈ 406 K). The conductivities in the liquid region have been fitted to polynomials of the form $\kappa(X) = A(X) + B(X)(T - T_m) + C(X)(T - T_m)^2$, where T_m is the intermediate temperature of the measured temperature range and X , the mole fraction of KHSO₄. The possible role of this binary system as a catalyst solvent is also discussed. © 2005 Elsevier B.V. All rights reserved.

Keywords: NaHSO₄; KHSO₄; Thermodynamic properties; Conductivity; Phase diagram

1. Introduction

This paper reports the latest results of our ongoing research efforts on the chemistry of the active phase of the industrial SO₂ oxidation catalyst and derived model systems. The composition of the industrial catalyst for sulfuric acid production, which is also used for catalytic cleaning of flue gases, is the molten salt-gas system M₂S₂O₇/MHSO₄/V₂O₅–SO₂/O₂/SO₃/H₂O/N₂ (M = alkali). In traditional sulfuric acid production, the H₂O content is low, shifting the equilibrium $\text{H}_2\text{O} + \text{S}_2\text{O}_7^{2-} \leftrightarrow 2\text{HSO}_4^-$ to the left, while in wet flue gas this equilibrium is shifted towards the right, i.e. toward formation of hydrogensulfate. V₂O₅ dissolves in these melts and the vanadium complexes formed are essential for the catalytic activity of the system. To understand the mechanism of the catalytic oxidation of SO₂, we have previously explored the vanadium chemistry (see [1–5] and references therein) and the phase diagrams of K₂S₂O₇–V₂O₅ [1] Rb₂S₂O₇–V₂O₅ [2], Cs₂S₂O₇–V₂O₅ [3,4] and M₂S₂O₇–V₂O₅ (M = 80%K + 20%Na) [5]. We have previously characterized the solvents M₂S₂O₇ and MHSO₄ (M = Na, K, Rb and Cs) and constructed phase diagrams of the binary systems Na₂S₂O₇–

NaHSO₄ [6], K₂S₂O₇–KHSO₄ [7], Cs₂S₂O₇–CsHSO₄ [8], and Na₂S₂O₇–K₂S₂O₇ [9]. A study of the NaHSO₄–KHSO₄ binary system by conductivity and the enthalpy of mixing is presented here, and finally calculation of the binary phase diagram [10,11]

2. Experimental

2.1. Chemicals

NaHSO₄ and KHSO₄ (Merck, Suprapur, 99) were dried at 110 °C and stored in sealed ampules in a glove box.

2.2. Thermodynamic and thermal measurements

The calorimeter used in this work consists primarily of a Tian-Calvet low temperature calorimeter [12,13]. The enthalpy of mixing of the NaHSO₄–KHSO₄ melts was measured by the breaking ampule method. The melts were contained in a fragile pyrex ampule. Mixing was carried out by breaking the ampules in the crucible in the calorimeter after complete thermal equilibration of all materials. Calibration of the calorimeter was performed after each experiment by dropping pure gold samples into the cell.

Differential thermal analysis was used to observe the phase transitions for the pure salts as well as the mixtures and to check

* Corresponding author. Tel.: +45 45252389.

E-mail address: rf@kemi.dtu.dk (R. Fehrmann).

the phase diagram obtained by conductivity. The DTA has been described previously [14].

2.3. Conductivity measurements

The experimental details concerning the borosilicate cell with two gold electrodes, sealed vacuum tight into the bottom of the cells, have been described earlier [15]. The cell was placed at the measuring temperature in an aluminium block furnace, regulated within 0.1 K, at the highest measuring temperature. The conductivity was then measured during stepwise decrease of the temperature until crystallization occurred, usually after subcooling of the melt. Thereafter, a new series of measurements were obtained by stepwise increase of the temperature. The eutectic temperature was identified by a drastic increase in the conductivity occurring when the system transforms from a solid phase into a two-phase system. The liquidus point was thereafter observed at the temperature where the conductivity coincided with the conductivities obtained during the decrease of temperature. The temperature was increased in small steps, i.e. 0.5–2 °C close to the phase transition temperatures and 5–10 °C far from these, until the initial high temperature of the melt was reached and the reproducibility of the conductivity was checked. The conductivity was measured by a Radiometer CDM-230 conductivity-meter. The temperatures were obtained by chromel–alumel thermocouples calibrated against a Pt 100 resistance thermometer and placed directly at the capillary tube of the conductivity cell. Cell constants, of the order of 100–200 cm⁻¹, were found by measuring the conductivity of KCl standard solutions at ambient temperature as previously described [16].

3. Results and discussion

3.1. Enthalpy of mixing of NaHSO₄–KHSO₄

The enthalpy of liquid–liquid mixing of the NaHSO₄–KHSO₄ binary system at $T=505$ K is displayed in Fig. 1. $\Delta_{\text{mix}}H$ was

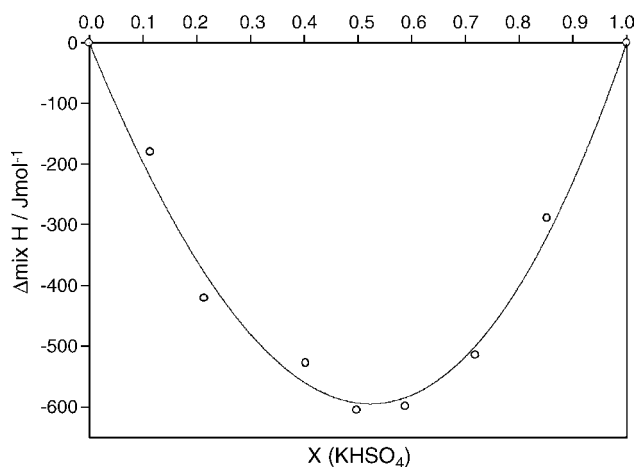


Fig. 1. Liquid–liquid molar enthalpies of mixing, $\Delta_{\text{mix}}H$, of the NaHSO₄–KHSO₄ system at 505 K. The fitted curve corresponds to $\Delta_{\text{mix}}H = X(1 - X)(-2156 - 438X)$, where X is the mole fraction of KHSO₄.

fitted to (1)

$$\Delta_{\text{mix}}H = X(1 - X)(A + BX) \quad (1)$$

where X is $X(\text{KHSO}_4)$; $A = -2156 \text{ J mol}^{-1}$; and $B = -438.2 \text{ J mol}^{-1}$. The minimum of this function representing $\Delta_{\text{mix}}H$ versus $X(\text{KHSO}_4)$ is found at $X(\text{KHSO}_4) = 0.523$, $\Delta_{\text{mix}}H = -595 \text{ J mol}^{-1}$. These values deviate from those found in [10] that were measured by the drop method, due to the drop method being inaccurate for small enthalpies of mixing, i.e. the error is of the same order of magnitude as the measured quantity. So, the breaking ampoule method was chosen, because it is more suitable for measuring small reaction enthalpies, giving a direct measurement of $\Delta_{\text{mix}}H$.

3.2. Phase diagram of the NaHSO₄–KHSO₄ system

The conductivity, κ , of the solid and molten mixtures of the NaHSO₄–KHSO₄ binary system were measured at 10 different compositions spanning the entire composition range. The temperature ranges from the completely molten state at 503–393 K, below the melting temperature of the eutectic. The results of the conductivity measurements are plotted as $\ln(\kappa)$ versus $1000/T$ in Fig. 2. A marked change in the conductivity of the mixture is found for several compositions at the solidus temperatures and less dramatic breaks are observed at the liquidus temperature, except for the pure compounds NaHSO₄ and KHSO₄, where the change in conductivity is steep upon melting, since no two-phase regions are present. The transition temperatures are listed in Table 1. The solidus temperatures for mixtures of NaHSO₄ and KHSO₄ are equal to the temperature of fusion of the eutectic. This is similar to what was observed earlier for analogous systems [6]. The temperature was not decreased sufficiently to observe the solidus transition for $X(\text{KHSO}_4) = 0.8007$, due to the increased risk of breaking the cell, because of the different

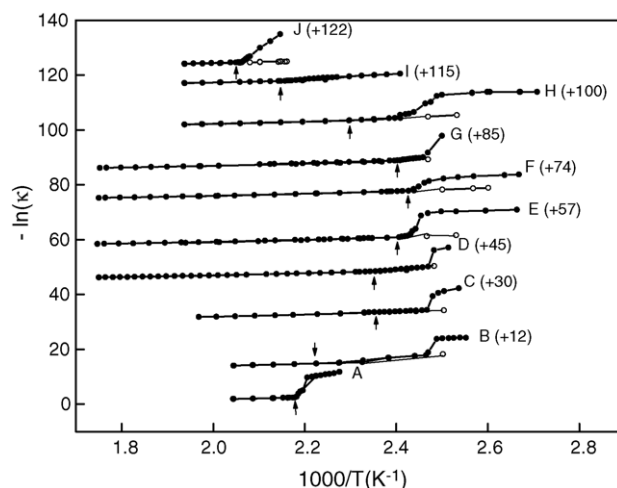


Fig. 2. Electrical conductivity, κ , vs. $1000/T$ for the NaHSO₄–KHSO₄ system at various compositions $X(\text{KHSO}_4)$: (A) 0.0000; (B) 0.1621; (C) 0.2993; (D) 0.3047; (E) 0.4081; (F) 0.4502; (G) 0.5035; (H) 0.5999; (I) 0.8007; (J) 1.0000. The curves are offset by the specified values (in parenthesis) for clarity. Open circles indicate subcooling and arrows indicate liquidus temperatures.

Table 1

Liquidus and solidus temperatures of the NaHSO₄–KHSO₄ system from conductivity measurements at the indicated compositions

$X(\text{KHSO}_4)$	T_{sol} (K)	T_{liq} (K)
0.0000		458
0.1621	405	439
0.2993	403	425
0.3047	403	425
0.4081	408	415
0.4502	406	412
0.5035	405	415
0.5999	406	435
0.8007		466
1.0000		488

thermal expansion coefficients of the pyrex glass of the cell and the solids formed.

The NaHSO₄–KHSO₄ binary system has also been investigated by DTA measurements on the compositions $X(\text{KHSO}_4) = 0.3008, 0.6012, 0.7023$ and 0.8007 . The samples were maintained at 383 K for 60 days in order to equilibrate them before analysis.

No thermal effects occur below 400 K. Except for the sample with $X(\text{KHSO}_4) = 0.8007$, all the thermograms present a series of random overlapped peaks between 405 and 425 K. This behaviour is explained by some particularities of the liquid hydrogensulfates. In the conductivity measurements, bubbles appeared in the liquids. To keep the samples completely liquid during the resistance measurements, the furnace and the cell had to be rotated and shaken until the bubbles disappeared. This procedure could not be applied in the DTA apparatus. Upon removing the sealed vials from the measurement cell, several small pieces of solids were stuck to the inner side of the vial at various heights. These small pieces had various sizes and were located at various distances from the temperature sensor in a finger at the bottom of the vial. As the temperature reached 406 K, all the solid spots begin to melt. The initial base line then rises to the endothermic side. The smallest particles are liquified before the bigger ones and the spots closest to the temperature sensor give the biggest peaks in the thermogram. This melting range may be so large that the thermal effect of the liquidus is difficult to see. This is the case for the $X(\text{KHSO}_4) = 0.3008$ thermogram, where the liquidus effect is small, and the $X(\text{KHSO}_4) = 0.6012$ thermogram, where it is probably hidden. Apparently, for the composition $X(\text{KHSO}_4) = 0.8007$, one uniform solid is present (see Fig. 3). For this sample, after the fusion has started, the base line rises towards the endothermic side, corresponding to the dissolution of KHSO₄ in the NaHSO₄–KHSO₄ melt. The break in the slope at 451–454 K shows the beginning of the transformation $\alpha\text{-KHSO}_4(\text{s}) \rightarrow \beta\text{-KHSO}_4(\text{s})$. At the end of this effect a new dissolution process occurs, i.e. the $\beta\text{-KHSO}_4(\text{s})$ dissolution in the NaHSO₄–KHSO₄ melt. For all the samples, the detected transitions confirm the data obtained by the conductivity measurements.

On the basis of the heats of mixing, the heats and temperatures of fusion and the heat capacities of the solid and the liquid hydrogensulfates found here or published elsewhere [6,7,10],

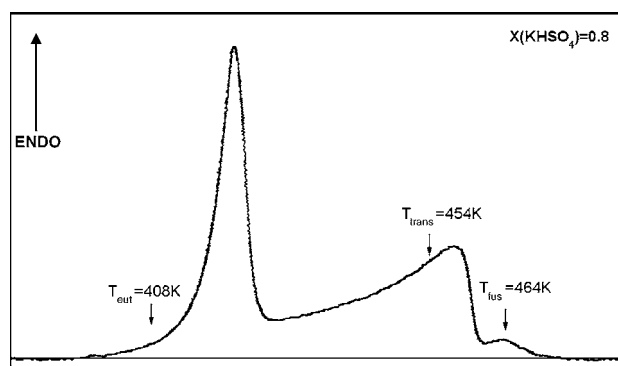


Fig. 3. Differential thermal analysis (DTA) of the NaHSO₄–KHSO₄ system for the composition $X(\text{KHSO}_4) = 0.8007$.

the solid–liquid phase transition over the entire composition range has been calculated. A classical method for optimizing the thermodynamic functions based on the equality of the chemical potentials of each component in the liquid and solid states was used. From this relation we obtain :

$$-\Delta G_{\text{fus}}^0(i) = RT \ln X_i^l + \Delta \bar{G}_i^{\text{xs}} \quad (2)$$

where X_i^l and $\Delta \bar{G}_i^{\text{xs}}$ represent the molar fraction and the excess molar Gibbs free energy of component i in the liquid state, respectively. By considering the liquid solution as regular, the calculations give a very low melting temperature of the eutectic, in accordance with the only other published [11] values for the NaHSO₄–KHSO₄ eutectic : $X(\text{KHSO}_4) = 0.455$ melting at $T = 395$ K. We have then introduced an excess term in our calculations which allows fitting all the experimental points together:

$$\Delta S^{\text{ex}} = WX(1 - X) \quad (3)$$

Here W is estimated to be : $-5 \text{ J mol}^{-1} \text{ K}^{-1}$. So, the excess Gibbs free energy in the liquid state could be expressed by the

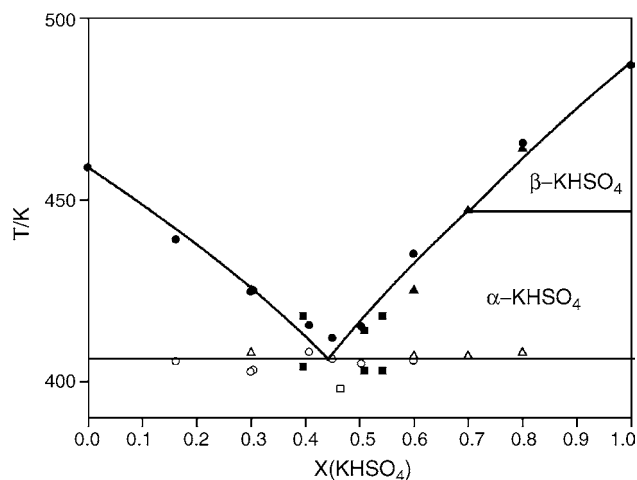


Fig. 4. Phase diagram of the NaHSO₄–KHSO₄ system based on conductivity measurements (circles) and thermal measurements (triangles). Open symbols indicate the solidus line (temperature of fusion of the eutectic). The liquidus line and composition and melting point of the eutectic mixture are calculated as described in the text. Values from the literature (solid squares) [10] and (open square) [11].

Table 2

Liquidus temperatures, T_{liq} , middle temperatures, T_m and coefficients for empirical equations^a for the specific conductivity of different compositions of the molten NaHSO₄–KHSO₄ system in the measured temperature range^b

$X(\text{KHSO}_4)$	T_{liq} (K)	T_m (K)	$A(X)$ ($\Omega^{-1} \text{cm}^{-1}$)	$B(X)$ ($10^{-3} \Omega^{-1} \text{cm}^{-1} \text{deg}^{-1}$)	$C(X)$ ($10^{-6} \Omega^{-1} \text{cm}^{-1} \text{deg}^{-2}$)	S.D. ($\Omega^{-1} \text{cm}^{-1}$)
0.0000	459	468	0.10516	1.91	7.81	0.00031
0.1621	439	464	0.08045	-1.57	8.09	0.00057
0.2993	424	451	0.06097	-1.33	4.88	0.00200
0.3047	425	451	0.06352	1.51	4.70	0.00096
0.4081	415	477	0.08942	1.51	6.19	0.00148
0.4502	412	471	0.09110	1.60	6.70	0.00150
0.5035	415	474	0.07760	1.22	3.57	0.00255
0.5999	435	475	0.07561	1.35	5.72	0.00140
0.8007	465	477	0.07109	1.17	0.91	0.00274
1.0000	488	489	0.07340	1.19	5.00	0.00058

^a $\kappa = A(X) + B(X)(T - T_m) + C(X)(T - T_m)^2$, $T \geq T_{liq}$ (T in Kelvin).

^b See Fig. 2 for the highest measuring temperature.

analytical expression :

$$\Delta G^{\text{ex}} = X(1 - X)(-2156 + 5T - 438.2X) \quad (4)$$

The final calculated phase diagram is shown in Fig. 4, with the eutectic values being $X(\text{KHSO}_4) = 0.44$ melting at $T = 406$ K, together with the experimental points. As reported earlier, the $\alpha \rightarrow \beta$ solid–solid transition for KHSO₄ was found at 451 K [7].

3.3. Conductivity of the NaHSO₄–KHSO₄ liquid

The conductivities of the 10 different compositions measured in the liquid region have been fitted as previously [7], to polynomials of the form $\kappa = A(X) + B(X)(T - T_m) + C(X)(T - T_m)^2$ where $T \geq T_{liquidus}$ and T_m is the middle temperature as given in Table 2 together with the polynomials and the standard deviations for the different compositions of the melt.

To show the variation of conductivity with composition, the κ isotherm at 489 K for all of the measured compositions is displayed in Fig. 5 and shows a steady decrease with increasing content of KHSO₄ in the melt, as expected from displacement of the smaller and more mobile Na⁺ ion by the larger K⁺ ion. This tendency was also observed previously [9] for the Na₂S₂O₇–K₂S₂O₇ system.

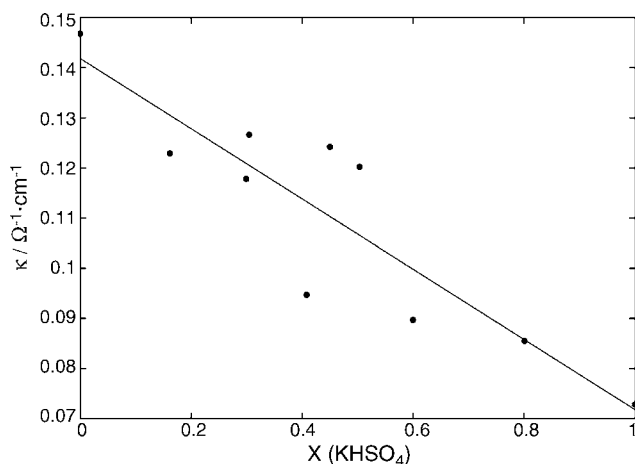


Fig. 5. Conductivity isotherm at 489 K for the NaHSO₄–KHSO₄ system, with curve fitting corresponding to, $\kappa = 0.142 - 0.0700X \Omega^{-1} \text{cm}^{-1}$.

4. Relation to catalysis

The traditional sulfuric acid catalyst consists of V₂O₅ promoted by a mixture of K (80%) and Na (20%) salts, e.g. as sulfates. The molar ratio of vanadium to total alkali is typically 3.8 and this catalytically active mixture is mixed with a porous Kieselguhr (SiO₂) carrier material. Pellets are then extruded, so the pores become partly filled with molten pyrosulfates, which are formed at 400–600 °C during activation of the reaction $\text{SO}_2 + 1/2\text{O}_2 \rightleftharpoons \text{SO}_3$, followed by $\text{SO}_3 + \text{SO}_4^{2-} \rightleftharpoons \text{S}_2\text{O}_7^{2-}$. This solvent is then partly transformed to a mixture of $\text{S}_2\text{O}_7^{2-}$ and HSO_4^- , depending on the water vapor pressure in the gas. At low temperatures and relatively high water partial pressures, the transformation to hydrogensulfate may be complete and according to the phase diagram in Fig. 4, the melting point of the catalyst solvent decreases to around 463 K for the traditional composition NaHSO₄(20%)–KHSO₄(80%). From this phase diagram (Fig. 4), it can also be concluded that the lowest possible melting point is 406 K, obtained for the composition NaHSO₄(56%)–KHSO₄(44%). This looks very promising for the creation of the long sought low temperature SO₂ oxidation catalyst. However, the solubility of V(V) complexes, the degree of reduction of V(V) to V(IV) and V(III) by SO₂, the solubility of the lower oxidation state vanadium compounds, the dew point of sulfuric acid and the kinetics of the catalyzed reaction in this melt at these low temperatures are of concern before such a drastic change in composition and process conditions can be proposed.

References

- [1] G.E. Folkmann, K.M. Eriksen, R. Fehrmann, M. Gaune-Escard, G. Hatem, O.B. Lapina, V.V. Terskikh, J. Phys. Chem. B 102 (1998) 24.
- [2] F. Abdoun, G. Hatem, M. Gaune-Escard, K.M. Eriksen, R. Fehrmann, J. Phys. Chem. B 103 (1999) 3559.
- [3] G.E. Folkmann, Ph.D. Thesis, Chemistry Department A, 1991, The Technical University of Denmark, Lyngby.
- [4] G.E. Folkmann, G. Hatem, R. Fehrmann, M. Gaune-Escard, N.J. Bjergerum, Inorg. Chem. 32 (1993) 1559.
- [5] D.A. Karydis, S. Boghosian, R. Fehrmann, J. Catal. 145 (1994) 312.
- [6] G. Hatem, M. Gaune-Escard, S.B. Rasmussen, R. Fehrmann, J. Phys. Chem. 103 (1999) 1027.

- [7] K.M. Eriksen, R. Fehrmann, G. Hatem, M. Gaune-Escard, O.B. Lapina, V.M. Mastikhin, *J. Phys. Chem.* 100 (1996) 10771.
- [8] S.B. Rasmussen, H. Hamma, O.B. Lapina, D.F. Khabibulin, G. Hatem, K.M. Eriksen, R.W. Berg, R. Fehrmann, *J. Phys. Chem. B* 107 (2003) 13823.
- [9] S.B. Rasmussen, K.M. Eriksen, G. Hatem, F. da Silva, K. Stahl, R. Fehrmann, *J. Phys. Chem. B* 105 (2001) 2747.
- [10] G. Hatem, K.M. Eriksen, R. Fehrmann, *J. Therm. Anal. Calorim.* 68 (2002) 25.
- [11] B.J. Meehan, S.A. Tariq, J.O. Hill, *J. Therm. Anal.* 12 (1977) 235.
- [12] E. Calvet, H. Prat, *Microcalorimétry, Applications Physico-chimique et Biologiques*, Masson ed., Paris, 1956.
- [13] E. Calvet, H. Prat, *Récents Progrès en Microcalorimétrie*, Dunod ed., Paris, 1958.
- [14] T. Jriri, *L'étude Thermodynamique des Systèmes Binaires et Ternaires de Nitrates Alcalins*, Université de Provence, Aix-Marseille, Marseille, 1994.
- [15] K. Nielsen, R. Fehrmann, K.M. Eriksen, *J. Inorg. Chem.* 23 (1993) 4714.
- [16] G. Hatem, R. Fehrmann, M. Gaune-Escard, N.J. Bjerrum, *J. Phys. Chem.* 91 (1987) 197.